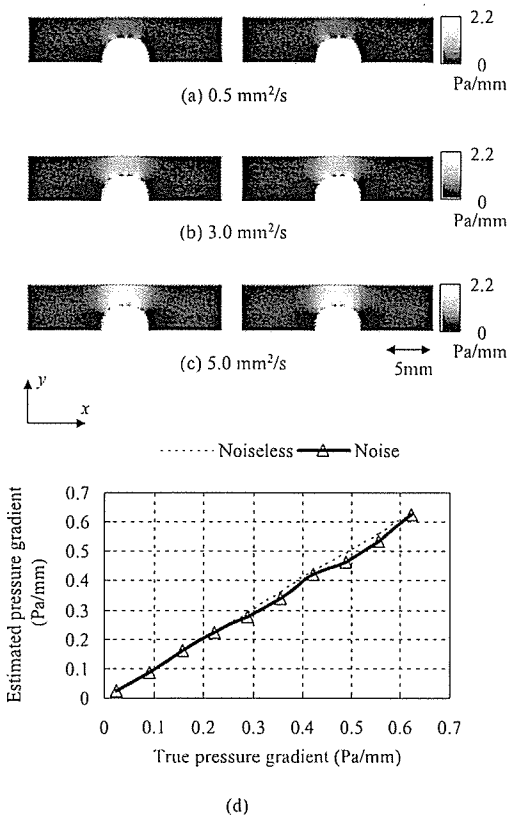

(d)

Fig. 7. Tangential pressure gradient estimation along the streamline. In (a) to (c), left panels indicate the ideal tangential pressure gradients obtained using the velocity vector distributions without noise, and right panels indicate the estimated tangential pressure gradients obtained using the velocity vector distributions with noise. (d) True and estimated values of the tangentinal pressure gradients. Horizontal axis indicates the true values and the vertical axis indicates the estimated pressure gradient values.

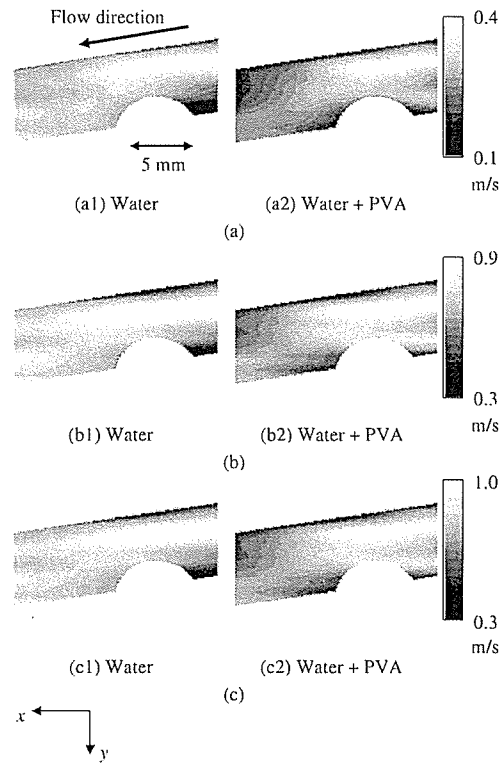

Fig. 8. Results of 2D velocity vector measurements. Left panels show the results for water and right panels show the results for water mixed with PVA. (a) Beam axis component. (b) Estimated lateral component. (c) Absolute values of velocity vector. Maximum and minimum values of each vector component along the axes on the *xy* coordinate system are assigned as white and black pixels, respectively.

tween the ideal (true) and the estimated tangential pressure gradients. The horizontal axis indicates the true values and the vertical axis indicates the estimated pressure gradient values. Here, the broken line indicates the estimated result when the ideal velocity vector distributions without noise were applied, and the solid line indicates the estimated result when the velocity vector distributions with noise were applied. This figure also shows that the estimated values coincide well with the true values. From these results, it was confirmed that the proposed method can be used to estimate a valid tangential pressure gradient when the velocity vector distributions can be accurately obtained.

4. Experimental Data Analysis

To verify the validity of the proposed method empirically, data obtained in a flow phantom experiment were analyzed. In the experiment, the same setup as that in a previous work[8] was applied. Here, a brief explanation of the setup is described.

Similar to the simulation analysis, a step imitating the plaque structure was placed on the inner wall of a silicone tube with a diameter of 5 mm, to generate the velocity vector field. Two fluid types, water and water mixed with poly(vinyl alcohol) (PVA), were prepared. The kinematic viscosity coefficient increases upon mixing PVA with water. As a result of the measurement with a viscometer, the kinematic viscosity coefficients of water and water mixed with PVA were found to be 1.5 and 6.2 mm^2/s, respectively, at the temperature of 21 °C. Rice powder was mixed into each type of fluid to cause the ultrasonic scattering. These fluids flowed through the tube at a speed of 1.0 m/s as a steady flow, and the temperature of fluids was kept at 21 °C. The tube was placed in a water tank, and the ultrasonic probe for measuring the velocity was set at the top of the tube at a distance of 50 mm from the center axis of the tube. The angle between the central tube axis and the ultrasonic beam direction was set to 67°.

The ultrasonic probe was driven at a center frequency of 4.7 MHz. The beam axis velocity profile was measured by the autocorrelation method in the Doppler method, using the echo train data obtained by transmitting 74 pulses in the same direction. The beam axis velocity distribution, which is composed by 20 scan lines, was obtained by scanning the probe horizontally with the stepping motor drive.

Lateral velocity component, which is orthogonal to the beam axis component, was obtained by applying a method utilizing the incompressible condition, as in the previous work.[8]

The 2D velocity vector distributions on the central cross section of the tube, obtained by the above-described process, are shown in Fig. 8 for (a) the beam axis component, (b) the estimated lateral component and (c) the absolute values of the velocity vector. Left panels show the results for water

and right panels show the results for water mixed with PVA. The kinematic viscosity coefficient is estimated using these velocity vector distributions, and furthermore, the mutually perpendicular pressure gradients determined by probe positioning are estimated; ultimately, the tangential pressure gradient distribution acting along the streamline is obtained. As a results of the kinematic viscosity estimated using the 2D velocity vector distributions shown in Fig. 8, the kinematic viscosity coefficients of water and water mixed with PVA were found to be 1.25 and 6.24 mm^2/s, respectively. These estimated values are close to the values measured with the viscometer, indicating valid results. Although the estimation for higher viscosity fluid exhibits higher accuracy than for lower viscosity fluid when comparing the ultrasonic estimations with the kinematic viscosity values measured with the viscometer, we believe that this accuracy is not universal. In this experiment, the accuracies of the velocity vector measurement for these two fluids are the same because these fluids flow in the tube at the same speed. Although there locally exist regions of lower velocity and the flow pattern becomes complex in the higher viscosity fluid, it is predicted that the same accuracies can be obtained for the kinematic viscosity estimation because all flow speeds are the same and the kinematic viscosity coefficient is calculated as an average around the stenosis. As the reason behind the occurrence of the difference between the estimation accuracies, various factors, such as a statistically insufficient number of experimental data and viscosity fluctuations due to the minute variations of the fluid temperature, might be given. Although the statistical tendency of the kinematic viscosity estimation must be assessed in the future, it can at least be considered that a valid estimation was accomplished in this study, because the kinematic viscosity estimation can be performed with good accuracy and the two fluids can be discriminated on the basis of the estimated kinematic viscosity coefficients.

When the central difference method is directly applied to the velocity vector distribution including fluctuation due to noise, as shown in Fig. 8, the accuracy of the pressure gradient distribution decreases because the noise is amplified due to the high-order derivative term calculation. In order to suppress the errors due to difference operation and to stabilize the calculations of the pressure gradient distribution, each distribution of the velocity vector components was interpolated by the polynomial approximation technique and differentiated by the central difference method. When applying the polynomial approximation, it is important to determine its order. In this study, different orders were used when each velocity component distribution was approximated by the polynomial approximation along x and y directions, because these velocity profiles along the x and y directions are different from each other.

First, the y direction almost corresponds to the radial direction of the tube, because of the tube placement. If the flow is laminar, the velocity profile along the radial direction becomes a parabolic curve. Consequently, u and v profiles along the y direction can also be approximated as a parabolic curve. In this experiment, although the tube does not have a uniform diameter because it includes the step, if the conditions for laminar flow are satisfied, the velocity profile along the y direction can also be approximated as a parabolic curve. Therefore, the conditions for laminar flow in this experiment were evaluated using the Reynolds number, which is defined as $U_m D/\nu$, where U_m, D, and ν are the mean velocity, the tube diameter, and the kinematic viscosity coefficient, respectively. Since this tube structure is divided into the stenosed part and the non-stenosed part, Reynolds numbers at each part for water and water mixed with PVA were calculated by substituting the values of the measured mean velocity, the diameter at each part and the kinematic viscosity coefficient measured with the viscometer into the definition of the Reynolds number. As a consequence, the Reynolds numbers were 1666 at the non-stenosed part and 2000 at the stenosed part in water, and 403 at the non-stenosed part and 483 at the stenosed part in water mixed with PVA. In general, since the critical Reynolds number is about 2000 in the tube,[11] the flow patterns in this experiment can be roughly approximated as a laminar flow. Therefore, the order of the polynomial approximation along the y direction was set to be 2, because it is expected that the velocity profile along the y direction would be close to a parabolic curve.

The order of the polynomial approximation along the x direction is determined to reduce the difference between the polynomial approximation and the actual measured distributions because there is no *a priori* information such as the parabolic curve. In order to determine this order, the polynomial approximations were performed changing the orders up to 7, and the errors were evaluated, as shown in Fig. 9. Naturally, although the higher order causes the approximation accuracy to increase, error updating in all curves shown in Fig. 9 almost reaches a plateau above the 5th order. This result indicates that 5th or higher order polynomial approximation along the x direction is valid for these experimental data. In order to achieve more accurate approximation, 7th-order polynomial approximation was used for the interpolation along the x direction. For the above determination of the order and the polynomial approximation, the interpolated 2D velocity vector distributions are shown in Fig. 10. On the whole, although the velocity distributions shown in Fig. 8 are smoothed by the

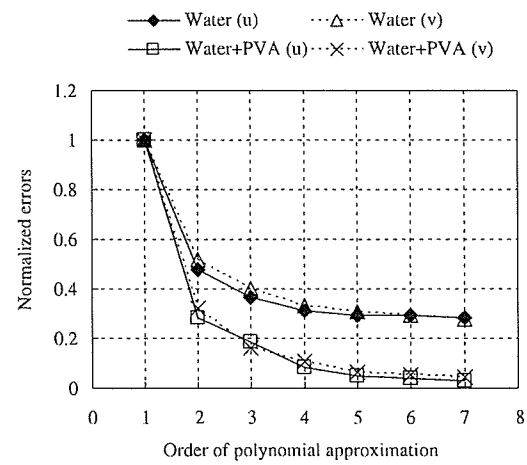

Fig. 9. Relationship between the orders of polynomial approximation and the normalized errors of the polynomial approximation along x directions for u and v distributions in water and water mixed with PVA.

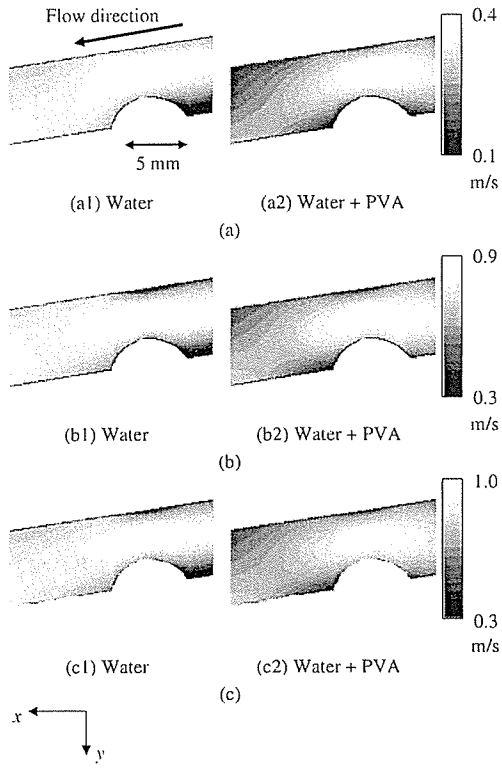

Fig. 10. Incorpolated 2D velocity vector distributions by the polynomial approximation method. Seven orders of polynomial approximation were set for the lateral direction and 2 orders for the beam-axis direction. Left panels show the results for water and right panels show the results for water mixed with PVA. (a) Beam axis component. (b) Estimated lateral component. (c) Absolute values of the velocity vector. Maximum and minimum values of each vector component along the axes on the xy coordinate system are assigned as white and black pixels, respectively.

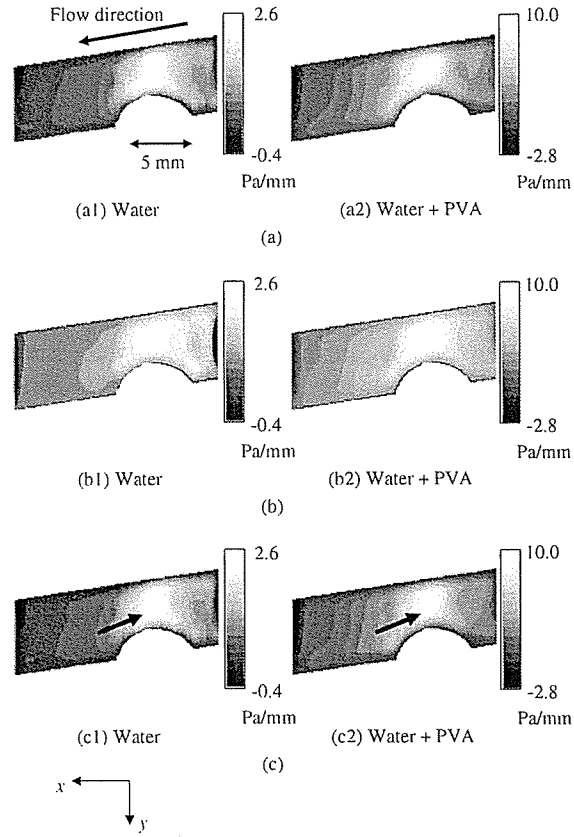

Fig. 11. Results of the pressure gradient estimation based on the velocity vector distribution. Left panels show the results for water and right panels show the results for water mixed with PVA. (a) x and (b) y components of the pressure gradients on the xy coordinate system. (c) Estimated tangential pressure gradient along the streamline. In (a) and (b), maximum and minimum values of each gradient component along the axes on the xy coordinate system are assigned as white and black pixels. In (c), maximum and minimum values of the tangential pressure gradient along the streamline are assigned as white and black pixels.

polynomial approximation, Fig. 10 reflects the features in Fig. 8.

After interpolating the velocity vector distributions, the pressure gradient distributions were calculated by central difference operations with difference widths along the x and y directions set to 1 and 0.45 mm, respectively. Figure 11 shows the pressure gradient distribution obtained with the estimated kinematic viscosity coefficient and the velocity vector distribution. Left panels show the results for water and right panels show the results for water mixed with PVA. Figures 11(a) and 11(b) show the pressure gradient components obtained using eqs. (1) and (2), and these correspond to the x and y components of the pressure gradients on the xy coordinate system, respectively. However, these were governed by the probe position. That is, the x axis corresponds to the lateral direction, and the y axis corresponds to the beam axis direction. As mentioned in §2, the pressure gradient assessment based on probe position, that is, the angle between the beam and the flow axes, is not invariant. Figure 11(c) shows the estimated distribution of the tangential pressure gradient acting along the streamline. Similar to the simulation results, the valid result that the tangential pressure gradient around the step arrowed in Fig. 11(c) is larger than that in the other regions was observed. Thus, the tangential pressure gradient can be used to assess the property of the flow itself, independently of the probe position.

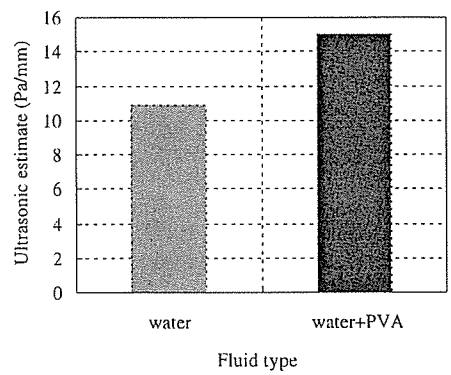

Fig. 12. Tangential pressure gradients around the step for the two types of fluid, water and water mixed with PVA. These were obtained as absolute values.

Figure 12 shows the averaged tangential pressure gradients around the step for the two fluids. These were obtained as absolute values. The average value for water mixed with PVA is slightly larger than that for water. Since the flow rate

was maintained almost constant, it is predicted that the pressure gradient is affected by the estimated kinematic viscosity coefficient, as in the simulation results. Therefore, these results indicate that the proposed method can be used to estimate a valid pressure gradient.

5. Conclusions

In this paper, with the aim of assessing the mechanical load applied to the vessel wall because of blood flow, a method for estimating the pressure gradient distribution was proposed. This method involves the previously reported method for estimating the kinematic viscosity coefficient.[8] The validity of the proposed method was investigated by analyzing the data obtained by computer simulation and the flow phantom experiment. The results indicated that the proposed method can be used to estimate a valid pressure gradient distribution.

In the future, it will be necessary to improve the robustness to noise when estimating the pressure gradient distribution, because this method is based only on velocity vector distributions. In particular, the robustness is an important factor in applications to the actual human blood flow state. In order to improve the robustness, it is promising to improve the velocity vector calculation and the derivative operation.

In addition to the above future work, simulations and experiments concerning various vascular situations, such as carotid bifurcation, will be conducted, and furthermore, the proposed method will be applied to in vivo experiments.

1) E. Falk, P. K. Shah and V. Fuster: Circulation **92** (1995) 657.
2) M. Luiza, C. Albuquerque and A. S. Flozak: Exp. Cell Res. **270** (2001) 223.
3) K. Nguyen, C. Patterson, M. Runge, S. Eskin and L. Mcintire: Proc. 1999 BMES/EMBS Conf., 1999, Vol. 1, p. 9.
4) Q. Yuchen and J. M. Tarbell: Proc. 1999 BMES/EMBS Conf., 1999, Vol. 1, p. 209.
5) J. Hanjoong and C. B. Yong: Proc. 2002 EMBS/BMES Conf., 2002, Vol. 1, p. 639.
6) M. F. Coughlin and G. W. Schmid-Schonbein: Proc. 2002 EMBS/BMES Conf., 2002, Vol. 1, p. 308.
7) S. Muller, V. Labrador, S. Legrand, X. Wang, D. Dumas and J. F. Stoltz: Proc. 1999 BMES/EMBS Conf., 1999, Vol. 2, p. 1340.
8) N. Nitta and K. Homma: Jpn. J. Appl. Phys. **44** (2005) 4602.
9) N. Nitta, K. Homma and T. Shiina: Proc. 2005 IEEE Ultrason. Symp., 2005, p. 520.
10) C. C-Bacrie: Proc. 1999 IEEE Ultrason. Symp., 1999, Vol. 2, p. 1489.
11) Y. C. Fung: *Biomechanics: Circulation* (Springer-Verlag, New York, 1996).

Appendix: Pressure Gradient Estimation in 3D Flow State

In the 3D flow state, the pressure gradient vector components in the Cartesian coordinate system can be derived, using the Navier-Stokes equations, as

$$\frac{\partial p}{\partial x} = \rho\left(\nu\nabla^2 u - \frac{Du}{Dt}\right), \tag{A·1}$$

$$\frac{\partial p}{\partial y} = \rho\left(\nu\nabla^2 v - \frac{Dv}{Dt}\right), \tag{A·2}$$

$$\frac{\partial p}{\partial z} = \rho\left(\nu\nabla^2 z - \frac{Dz}{Dt}\right), \tag{A·3}$$

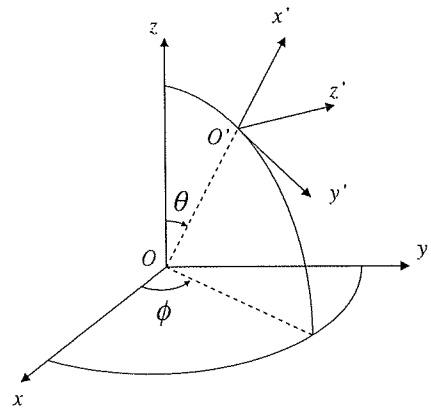

Fig. A·1. Coordinate transformation in a 3D space.

where ρ: density, ν: kinematic viscosity coefficient, u, v, w: velocity vector components, ∇^2: Laplacian, and D/Dt: Lagrangian operator.

Equations (A·1)–(A·3) indicate that the pressure gradient components can be obtained using only velocity vector components under the assumption of a known density, because the kinematic viscosity coefficient can be calculated when attaining the velocity vector.

However, the above pressure gradients depend on the assignment of the Cartesian coordinate system. Therefore, as an independent assessment of the assignment of the coordinate system, it is promising for the pressure gradient to be calculated along the tangential direction of the streamline.

In the Cartesian coordinate system shown in Fig. A·1, the pressure gradient vector $(\partial p/\partial x, \partial p/\partial y, \partial p/\partial z)$ in the original O–xyz system can be transformed to the vector $(\partial p/\partial x', \partial p/\partial y', \partial p/\partial z')$ in the O'–$x'y'z'$ system, as follows:

$$\begin{pmatrix} \frac{\partial p}{\partial x'} \\ \frac{\partial p}{\partial y'} \\ \frac{\partial p}{\partial z'} \end{pmatrix} = \begin{pmatrix} \sin\theta\cos\phi & \sin\theta\sin\phi & \cos\theta \\ \cos\theta\cos\phi & \cos\theta\sin\phi & -\sin\theta \\ -\sin\phi & \cos\phi & 0 \end{pmatrix} \begin{pmatrix} \frac{\partial p}{\partial x} \\ \frac{\partial p}{\partial y} \\ \frac{\partial p}{\partial z} \end{pmatrix}. \tag{A·4}$$

In Fig. A·1, since the coordinate system is transformed such that the x' axis agrees with the tangential direction of the streamline, the tangential pressure gradient can be obtained as follows:

$$\frac{\partial p}{\partial x'} = \frac{\partial p}{\partial x}\sin\theta\cos\phi + \frac{\partial p}{\partial y}\sin\theta\sin\phi + \frac{\partial p}{\partial z}\cos\theta. \tag{A·5}$$

The rotation angles ϕ and θ are obtained from the velocity vector. In Fig. A·1, when the x' axis agrees with the velocity vector direction, both the v' component along the y' axis and the w' component along the z' axis become zero in the transformed O'–$x'y'z'$ system. Applying this relationship, eq. (A·5) is reduced to eq. (A·6) using the velocity vector components.

$$\frac{\partial p}{\partial x'} = \frac{\partial p}{\partial x}\frac{u}{V} + \frac{\partial p}{\partial y}\frac{v}{V} + \frac{\partial p}{\partial z}\frac{w}{V}. \tag{A·6}$$

Here, V is the absolute value of the velocity vector and is defined by $V = \sqrt{u^2 + v^2 + w^2}$. This means that the tangential pressure gradient can also be derived using the pressure gradient vector and the velocity vector in the original coordinate system, without cumbersome calculations of the rotation angles ϕ and θ, even when the complex 3D flow state is considered.

Original Article

Association of Genetic Variation of the Adiponectin gene with Body Fat Distribution and Carotid Atherosclerosis in Japanese Obese Subjects

Yuko Katsuda[1], Akimichi Asano[1], Yuko Murase[1], Daisuke Chujo[1], Kunimasa Yagi[1], Junji Kobayashi[2], Hiroshi Mabuchi[2], and Masakazu Yamagishi[1]

[1]Molecular Genetics of Cardiovascular Disorders, Graduate School of Medical Science, Kanazawa University, Kanazawa, Japan.
[2]Department of Lipidology, Graduate School of Medical Science, Kanazawa University, Kanazawa, Japan.

Aim: The aim of this study was to investigate the effect of SNP45 of the adiponectin gene on body fat distribution and carotid atherosclerosis in Japanese obese subjects.
Methods: A total of 64 obese subjects were investigated. Genotypes of SNP45 were assayed by polymerase chain reaction-restriction fragment length polymorphism. Visceral fat area (VFA) and subcutaneous fat area (SFA) were measured using computed tomography. The progression of atherosclerosis was evaluated by plaque score (PS) of carotid artery using B-mode ultrasonography.
Results: Men carrying the G allele of SNP45 showed higher VFA (172.8 ± 50.8 vs. 147.1 ± 58.7, $p = 0.005$), lower SFA (209.9 ± 101.8 vs. 273.4 ± 142.2, $p = 0.007$), higher VFA/SFA (V/S) ratio (1.00 ± 0.46 vs. 0.60 ± 0.26, $p < 0.001$) and higher PS (9.5 ± 3.7 vs. 6.8 ± 4.2, $p = 0.012$) than those with TT genotype. Multivariate analysis showed that SNP45 was an independent determinant of V/S ratio and PS in men. In subgroup analysis, PS tended to be associated with V/S ratio only in the carrier of 45G allele.
Conclusion: These results suggest that the G allele could be a risk factor of metabolic syndrome and the development of atherosclerosis in Japanese obese subjects.

J Atheroscler Thromb, 2007; 14:19-26.

Key words; Visceral obesity, Plaque score, Polymorphism, PCR-RFLP

Introduction

Adiponectin is a 244-amino acid protein synthesized and secreted exclusively by adipose tissue[1, 2] and plays an important role in the regulation of energy homeostasis and insulin sensitivity[3-5]. Adiponectin also has anti-atherogenic effects. This protein has been shown to suppress the expression of class A scavenger receptors in macrophages, affect the nuclear factor (NF)-κB pathway and inhibit monocyte adhesion to aortic endothelial cells[6-8].

Address for correspondence: Yuko Katsuda, Molecular Genetics of Cardiovascular Disorders, Graduate School of Medical Science, Kanazawa University, 13-1 Takaramachi, Kanazawa 920-8640, Japan.
E-mail: y-katsuta@houju.or.jp
Received: May 23, 2006
Accepted for publication: October 14, 2006

Genetic variations in the human adiponectin gene, especially two single nucleotide polymorphisms (SNPs) (+45T>G and +276G>T), have been reported to be associated with obesity, insulin resistance[9], type 2 diabetes[10, 11], and coronary artery disease[12]. Hara *et al.* reported that these two SNPs were associated with insulin resistance, indicating the pathogenesis of type 2 diabetes[11]. The mechanism underlying insulin resistance in type 2 diabetes is not fully understood, but many studies in nondiabetic populations have addressed the importance of upper body fat distribution. However, the association between these SNPs and body fat distribution has not been investigated. Based on these previous findings, it has recently been reported that the G allele of SNP45 was associated with susceptibility to coronary artery disease independent of conventional risk factors[12]. Although, the mechanism is not clear, we hypothesized that SNP45 could modify body

fat distribution and lead to more accumulation of visceral adipose tissue, resulting in metabolic abnormalities and the development of atherosclerosis in the process of increasing adipose tissue. To determine the validity of this hypothesis, we investigated the association of SNP45 with (1) various clinical and metabolic parameters, (2) body fat distribution, and (3) the progression of atherosclerosis using the plaque score of the carotid artery and maximum IMT in a group of Japanese obese patients.

Material and Methods

Subjects

Sixty-four Japanese obese subjects (40 men and 24 women, aged 54.2 ± 16.6 years, BMI 30.3 ± 5.3 kg/m^2), receiving medical checkups in our institute from 2002 to 2004, were recruited for this study. These included 49 patients with type 2 diabetes, among whom 24 were treated with oral hypoglycemic agents, 13 with insulin, and 12 with diet alone. Subjects with other endocrine diseases or significant renal or hepatic disease were excluded.

Obesity was defined as a body mass index (BMI) ≧25 kg/m^2, based on the criteria of the Japan Society for the Study of Obesity[13]. Diabetes mellitus was diagnosed according to World Health Organization criteria[14] and/or receiving treatment for diabetes mellitus. Informed consent was obtained from all subjects. This study was approved by the Ethics Committee of Kanazawa University.

Screening of Mutations in the Adiponectin gene

Genomic DNA was extracted from peripheral blood leukocytes using the standard procedure. Genotypes were determined at position 45 relative to the translation start site (corresponding to GenBank AB012163S1, 2, 3) by PCR, followed by allele-specific hybridization.

DNA fragments containing SNP45 (372 bp) were amplified by PCR from genomic DNA using primers 5'-GCAGCTCCTAGAAGTAGACTCTGCTG-3' and 5'-GGAGGTCTGTGATGAAAGAGGCC-3'. PCR products were incubated at 25℃ for 2 hours using *SmaI* (New England BioLabs Inc. UK). Digested products were separated by size on 3% agarose gel with ethidium bromide staining. The DNA segment from the G/G homozygote of SNP45 was digested into 209 and 163 bp fragments.

Laboratory Measurements

BMI was calculated as weight (in kilograms) divided by height (in meters) squared. Waist circumference at the umbilical level was measured in the exhalation phase of respiration while standing.

Venous blood samples were obtained after a 12-hour overnight fast. Serum total cholesterol (TC) and triglyceride (TG) were determined by enzymatic methods, and high-density lipoprotein cholesterol (HDL-C) levels were measured by a polyanion-polymer/detergent method. Serum immunoreactive insulin (IRI) was measured by enzyme-linked immunosorbent assay, blood glucose with the glucose oxidase method, and HbA_{1c} by high-pressure liquid chromatography. The insulin resistance index was calculated based on homeostasis model assessment (HOMA) [fasting glucose (mmol/L) × fasting insulin (μU/mL)/22.5][15]. Plasma adiponectin levels were measured with an enzyme-linked immunosorbent assay kit (Otsuka Pharmaceutical Co., Tokushima, Japan), and leptin was measured by radioimmunoassay.

Body Fat Distribution

All subjects underwent computed tomography (CT) at the umbilical level to measure the cross-sectional abdominal subcutaneous fat area (SFA) and visceral fat area (VFA) using Fat Scan (N2 System Corp, Osaka, Japan)[16]. The VFA/SFA ratio was calculated as visceral fat area divided by subcutaneous fat area.

Determination of Plaque Score and Max IMT

A high resolution B-mode ultrasonography unit (SS-A 370A; Toshiba; Tokyo) with a 7.5 MHz transducer was used to determine the plaque score of the carotid artery[17]. Carotid Intima-Media Thickness (IMT) was measured at each common carotid, carotid bulb, and internal carotid artery.

The maximum IMT (Max-IMT) was defined as the highest IMT value at any location in the near and far walls of the carotid arteries, including atheromatous plaques on both sides. We defined a plaque, focal IMT thickening, as an area where IMT ≧ 1.1 mm, and calculated the plaque score by totaling the maximum thickness of all plaques on the near and far walls of vessels in the scanned area[17].

Statistical Analysis

All data are shown as the mean ± SD. A chi-square test was used to confirm that the genotype frequency was in Hardy-Weinberg equilibrium and to compare differences. Continuous variables were compared by ANOVA after being adjusted for age, BMI, and sex. Univariate and stepwise regression analyses were employed to examine the association between the plaque score and clinical parameters. All statistical analyses were conducted with StatView 5.0 for Macintosh

Table 1. Genotype distribution and allele frequencies for the adiponectin gene SNP45

	SNP45 genotypes			Allele frequencie	
	T/T	T/G	G/G	T	G
n (%)	34 (53.1)	25 (39.1)	5 (7.8)	0.72	0.28
male (n =40)	23 (57.5)	13 (32.5)	4 (10.0)	0.74	0.26
female (n =24)	11 (45.8)	12 (50.0)	1 (4.2)	0.71	0.29

Table 2. Clinical characteristics according to adiponectin genotypes at position 45

	T/T	T/G+G/G	P
n (%)	34 (53.1%)	30 (46.9%)	
M/F	23/11	17/13	0.36
Age (years)	53±15	56±18	0.39
Type 2 diabetes (%)	73.5	73.3	0.98
BMI (kg/m^2)	30.7±6.3	29.4±3.6	0.56
Waist (cm)	103.3±14.2	103.2±13.0	0.37
HOMA-R	3.6±2.3	3.3±1.9	0.80
HbA_{1c} (%)	7.1±1.9	6.7±1.6	0.32
Total cholesterol (mg/dL)	211±35	204±43	0.44
Triglycerides (mg/dL)	152±104	151±82	0.80
HDL cholesterol (mg/dL)	46±10	45±13	0.35
Adiponectin (μg/mL)	5.5±2.3	6.8±4.5	0.26
Leptin (ng/mL)	10.8±6.4	14.1±12.3	0.07
Systolic blood pressure (mmHg)	131±19	135±20	0.34
Diastolic blood pressure (mmHg)	79±11	79±14	0.65
Subcutaneous fat area (cm^2)	275.4±127.5	246.5±94.6	0.32
Visceral fat area (cm^2)	140.5±56.6	151.1±51.0	0.06
V/S ratio	0.56±0.24	0.76±0.45	0.009
Max IMT	1.89±0.81	2.21±0.91	0.27
Plaque score	6.1±4.1	9.7±3.9	<0.001

NOTE. Values are the means±SD. Heterozygotes and homozygotes for minor alleles were combined for presentation.
Abbreviations: BMI=body mass index, HOMA-R=homeostasis model assessment of insulin resistance
*P values adjusted for age, sex, and body mass index.

(Abacus Concepts, Berkeley, CA). A P value of less than 0.05 was considered statistically significant. In stepwise analysis, an F value greater than 4 was significant.

Results

Genotypes and Allele Distribution of SNP45 of the Adiponectin gene

The genotype and allele frequencies of study subjects are shown in **Table 1**. Genotype distributions were in Hardy-Weinberg equilibrium at both loci, with T being the major allele. The frequency of the T allele of SNP45 was 72%, and the frequencies of the T/T genotype, T/G genotype, and G/G genotype were 53.1%, 39.1%, and 7.8%, respectively.

Clinical and Metabolic Characteristics of this Study According to SNP45 of the Adiponectin gene

Table 2 shows a comparison of clinical characteristics and body composition according to adiponectin genotypes. Subjects were divided into 45T/T homozygote and those carrying the G allele (45T/G and 45G/G).

No differences in sex, age, or the proportion with diabetes were observed between any groups. Plasma leptin levels tended to be higher in carriers of the 45G allele (10.8±6.4 vs. 14.1±12.3, P=0.07). Other variables (HbA_{1c}, plasma lipid, and plasma adiponectin levels) did not differ between these genotypes.

Table 3. Clinical characteristics according to gender

	men	women	*P*
n	40	24	
Age (years)	51 ± 16	60 ± 14	0.02
BMI (kg/m^2)	30.7 ± 6.3	29.4 ± 3.6	0.56
Waist (cm)	102.7 ± 13.7	104.2 ± 13.5	0.03
HOMA-R	3.6 ± 2.4	3.1 ± 1.3	0.76
HbA_{1c} (%)	6.7 ± 1.9	7.4 ± 1.5	0.14
Total cholesterol (mg/dL)	204 ± 40	216 ± 36	0.15
Triglycerides (mg/dL)	166 ± 108	132 ± 59	0.37
HDL cholesterol (mg/dL)	42 ± 9	53 ± 12	0.02
Adiponectin (μg/mL)	5.2 ± 2.5	7.6 ± 4.4	0.03
Leptin (ng/mL)	9.6 ± 9.2	16.8 ± 9.2	0.03
Systolic blood pressure (mmHg)	132 ± 19	135 ± 19	0.27
Diastolic blood pressure (mmHg)	80 ± 13	77 ± 9	0.65
Subcutaneous fat area (cm^2)	246.4 ± 129.1	287.6 ± 76.3	<0.001
Visceral fat area (cm^2)	158.0 ± 56.3	124.5 ± 43.1	0.002
V/S ratio	0.77 ± 0.41	0.47 ± 0.17	<0.001
Max IMT	2.09 ± 1.00	1.96 ± 0.61	0.18
Plaque score	8.1 ± 4.1	7.9 ± 5.0	0.41

NOTE. Values are the means ± SD. Heterozygotes and homozygotes for minor alleles were combined for presentation.
Abbreviations: BMI = body mass index, HOMA-R = homeostasis model assessment of insulin resistance
* *P* values adjusted for age and body mass index.

Table 4. Body fat distribution and PS according to adiponectin genotypes at position 45 in men and women

	men			women		
	T/T	T/G + G/G	*P*	T/T	T/G + G/G	*P*
VFA	147.1 ± 58.7	172.8 ± 50.8	0.005	126.7 ± 52.0	122.7 ± 36.1	0.763
SFA	273.4 ± 142.2	209.9 ± 101.8	0.007	279.8 ± 95.6	294.3 ± 58.8	0.091
V/S ratio	0.60 ± 0.26	1.00 ± 0.46	<0.001	0.49 ± 0.18	0.44 ± 0.16	0.262
PS	6.8 ± 4.2	9.5 ± 3.7	0.012	4.4 ± 4.0	10.8 ± 3.8	0.135

NOTE. Values are the means ± SD. Heterozygotes and homozygotes for minor alleles were combined for presentation.
Abbreviations: VFA = visceral fat area, SFA = subcutaneous fat area

Relationship between Genotypes and Body Fat Distribution

When we considered the VFA/SFA ratio as a marker of body fat distribution, it was significantly higher in carriers of the 45G allele (0.76 ± 0.45 vs. 0.56 ± 0.24, $P = 0.009$), whereas there were no associations between SFA and SNP45. VFA tended to be higher in carriers of the 45G allele than TT homozygote (151.1 ± 51.0 vs. 140.5 ± 56.6 cm^2, $P = 0.06$). Neither BMI nor waist circumference significantly differed between the two groups. Since there were sex differences in body fat distribution in this study (**Table 3**: men vs. women; VFA: 158.0 ± 56.3 vs. 124.5 ± 43.1, $P = 0.002$; SFA: 246.4 ± 129.1 vs. 287.6 ± 76.3, $P < 0.001$; V/S ratio: 0.773 ± 0.410 vs. 0.470 ± 0.176, $P < 0.001$), we performed separate analyses of the association between SNP45 and body fat distribution by sex (**Table 4**, **Fig. 1**). In men, SNP45 was associated with the VFA, SFA, and V/S ratio, whereas in women SNP45 was not associated with body fat distribution.

Furthermore, to evaluate the contribution of SNP45 to the V/S ratio in men, stepwise regression analysis was used (**Table 5**). Selected variables were age, BMI, SNP45, and adiponectin. The data showed that age, SNP45, and plasma adiponectin levels were independent determinants of the V/S ratio in men ($R^2 = 0.588$, $P < 0.0001$).

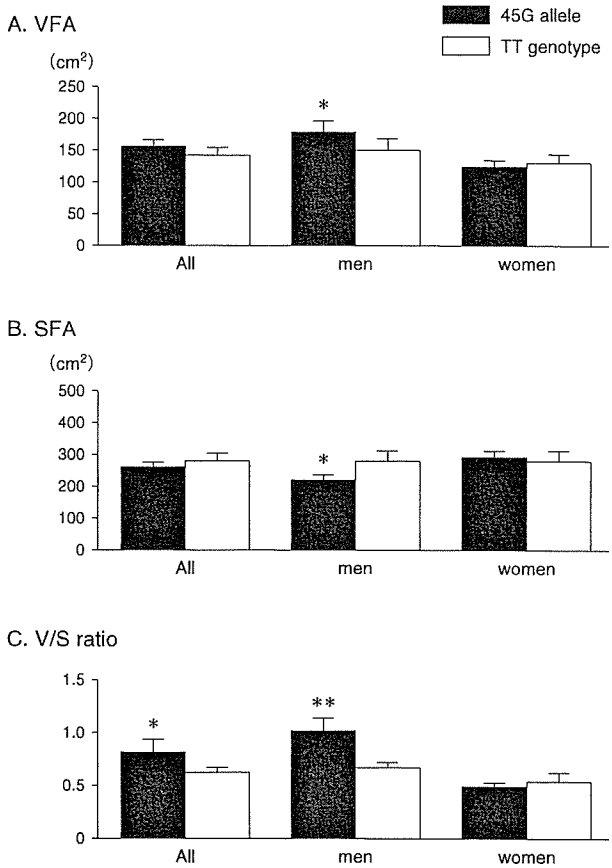

Fig. 1. Effect of SNP45 of the adiponectin gene on body fat distribution in all subjects, men and women

A. Effect of SNP45 on visceral fat area (VFA)
B. Effect of SNP45 on subcutaneous fat area (SFA)
C. Effect of SNP45 on VFA/SFA (V/F) ratio
Data are the means ± SE. $^{*}P<0.05$, $^{**}P<0.001$

Relationship between Genotypes and Plaque Score of Carotid Artery

We investigated the effect of SNP45 on the plaque score and max IMT of carotid arteries. Carriers of the G allele had significantly greater PS than TT genotype after adjusting for age, sex, and BMI (10.0 ± 3.7 vs. 6.4 ± 4.2, $P<0.001$).

As shown in **Table 4**, SNP45 was associated with PS in men, and PS of the G allele tended to be higher than the TT genotype in women. To analyze the independent contribution of SNP45 to PS in men, stepwise regression analysis was applied (**Table 6**). Selected variables were age, BMI, V/S ratio, adiponectin, TC, HDL-C, systolic BP, and SNP45. The data showed that age and SNP45 were independent determinant of PS in men ($R^2=0.372$, $P=0.0007$).

Table 5. Stepwise regression analysis for determinant of V/S ratio in men

Factor	β	F-value
Age	0.017	35.763
SNP45*	0.340	24.945
Adiponectin	−0.073	13.688

$R^2=0.588$
*TT genotype=0, TG genotype=1, GG genotype=2

Table 6. Stepwise regression analysis for determinant of PS in men

Factor	β	F-value
Age	0.143	13.362
SNP45*	2.509	7.563

$R^2=0.372$
*TT genotype=0, TG genotype=1, GG genotype=2

Table 7. Correlation of PS to V/S ratio according to the genotype in men and women

	equation	r	p
men			
all	y=4.05x+4.71	0.39	0.02
G allele	y=3.22x+6.17	0.38	0.14
TT genotype	y=2.91x+4.93	0.17	0.49
women			
all	y=4.67x+5.85	0.17	0.47
G allele	y=12.00x+5.41	0.60	0.06
TT genotype	y=−2.57x+5.59	0.13	0.75

Relationship between V/S Ratio and Plaque Score of Carotid Artery

To examine the effect of the V/S ratio on PS, we performed univariate analysis (**Table 7**).

There was a significant positive correlation between the V/S ratio and PS in men ($r=0.39$, $P=0.02$), whereas in women that correlation were not statistically significant ($r=0.17$, $P=0.47$).

Next, to investigate the impact of SNP45 on the association between the V/S ratio and PS, we subdivided into two groups according to the genotype of SNP45 in men and women. The V/S ratio tended to be associated with PS in the G allele in both men and women (men: $r=0.38$, $p=0.14$; women: $r=0.60$, $p=0.06$, respectively). In contrast, in subjects with the TT genotype, there was no relationship between the V/S ratio and PS.

Discussion

Our study had three major findings in Japanese obese subjects. First, SNP45 in the adiponectin gene was associated with body fat distribution. Second, SNP45 was associated with the development of carotid atherosclerosis. Moreover, SNP45 had an impact on the effect of visceral obesity for the progression of atherosclerosis. Third, there was a gender difference in the effect of SNP45.

First, we demonstrated that the G allele had higher VFA, lower SFA, and a significantly higher V/S ratio compared to the TT genotype in men. Multivariate regression analysis showed that SNP45 was an independent determinant of the V/S ratio. These results indicated that the G allele of SNP45 is a risky genotype of visceral adiposity, resulting in metabolic syndrome. To our knowledge, this is the first study to demonstrate the association of SNP45 with body fat distribution. Some reports have shown that SNP45 contributes to obesity, insulin resistance, or dyslipidemia[10, 18, 19]. In contrast, Ukkola *et al.* reported that SNP45 was found in equal frequency among obese and non-obese Swedish subjects[20]. In French Caucasians, the 45G allele frequency was similar in morbidly obese adults and control subjects[21]. The inconsistency between these reports suggested that SNP45 could not be associated simply with weight or prevalence of obesity, but might contribute to body fat distribution in the process of becoming obese. Since visceral adipose tissue is widely believed to play a key role in the pathogenesis of metabolic abnormalities, the G allele of SNP45 could be an independent risk factor for metabolic syndrome.

Second, another important finding of the present study was the significant association between SNP45 and carotid artery PS in men. A similar trend was observed in women. Multivariate regression analysis showed that SNP45 was an independent determinant of PS. These findings suggest that SNP45 may affect the development of carotid atherosclerosis not only by modulating visceral obesity but also by other pathways.

To the best of our knowledge, PS tends to be associated with the V/S ratio only in the G allele in both men and women. In a previous study, we described a strong association between the V/S ratio and carotid artery PS in Japanese males with metabolic syndrome[22], but patients with the TT genotype were protected from the atherogenic effect of visceral obesity. We hypothesized that visceral obesity might exaggerate the dysregulation of adiponectin properties of the G allele. The mechanism was unclear, but this hypothesis needs confirmation by expression studies.

Third, in this study the degree of the effect of SNP45 on body fat distribution and PS was different between men and women. Adipose tissue is sexually dimorphic in humans, with gender-specific differences in body fat distribution[23, 24]. Gonadal steroids are the major mediator of sex dimorphism of body composition in adults[25, 26]. Estrogen regulates both the metabolism and location of adipose tissue and plays a role in adipogenesis, adipose deposition, lipogenesis, lipolysis, and adipocyte proliferation[27]. Furthermore, in recent studies, Clegg *et al.* reported that gonadal steroids mediate body fat distribution and interact with the integrated adiposity messages conveyed to the brain[28]. Taken together with previous studies, our findings suggest that estrogen may interact with the adiponectin gene in adipocyte and modulate the effect of SNP45.

In addition, estrogen is known to have a cardioprotective effect. *In vivo* evidence suggests that the effect of estrogen on adhesion molecules is mediated by the inhibition of nuclear factor (NF)-κB DNA binding[29, 30]. As adiponectin has been shown to suppress the expression of class A scavenger receptors in macrophages, to affect the NF-κB pathway and to inhibit monocyte adhesion to aortic endothelial cells[6-8], atherogenic properties of the G allele may be suppressed by the effect of estrogen. Estrogen could interact with SNP45 and modulate the atherogenic function of adiponectin, but further large studies are needed to confirm the mechanism of gender-specific differences in the effect of SNP45.

The mechanistic relationship between SNP45 and both body fat distribution and the progression of atherosclerosis is unclear. SNP45 is located in exon 2 of the adiponectin gene and does not cause an amino acid change (GGT to GGG, Gly15Gly). One possibility is that SNP45 may have linkage disequilibrium with other undiscovered SNPs of the adiponectin gene having an effect on adiponectin expression, secretion, structure, or action. Another possibility is that SNP45 located in exon 2 is relatively close to the exon-intron boundary which may affect splicing machinery and effect adiponectin expression. The G allele of SNP45 may act through decreased adiponectin expression, which may cause increased visceral adipose tissue. Indeed, in Japanese type 2 diabetes, SNP45 is reported to be associated with reduced adiponectin levels[11]. Similar findings have been shown in an other study[31]. Furthermore, recent studies have reported various adiponectin functions as an adipocyte differentiation factor, helping to maintain equilibrium adipocyte size, as an autocrine/paracrine factor in adipose tissue and as a participating factor in the regulation of adipocyte metabolism and adipose tissue mass. In 3T3-L1 preadipocytes,

adiponectin overexpression accelerates cell proliferation and differentiation, while in mature adipocytes, autocrine adiponectin increases glucose uptake and lipid accumulation[32]. Transgenic overexpression of adiponectin in the physiological range induced morbid obesity without insulin resistance in ob/ob mice[21]. These reports indicated that hyperadiponectinemia may induce simple obesity with more subcutaneous fat accumulation, while decreased adiponectin levels may induce visceral obesity. Interestingly, the present study showed that hypoadiponectinemia was the third independent determinant of the V/S ratio. Due to these previous findings combined with our present study, the G allele might be genetically determined to have hypoadiponectinemia, contributing to the progression of visceral obesity. In contrast, the TT genotype might favor the accumulation of subcutaneous adipose tissue through hyperadiponectinemia, preventing insulin resistance, and eventually metabolic syndrome.

Adiponectin exists largely as low molecular weight (LMW) hexamers and high molecular weight (HMW) multimers[32, 33]. Recent article showed that the ratio of HMW to total adiponectin was responsible for metabolic effects[34]. Another study showed that HMW adiponectin was an important factor in metabolic syndrome[35]. Therefore, the alternative possibility of the atherogenic effect of SNP45 is that the proportion of HMW adiponectin might decrease in the G allele of SNP45, leading to atherosclerosis. As we measured total adiponectin and did not assess multimeric forms of adiponectin, further study is needed.

In conclusion, we demonstrated that SNP45 was associated with body fat distribution and PS of carotid arteries. The TT genotype is a protective genotype from metabolic syndrome and atherosclerosis progression in Japanese obese subjects. The mechanism by which SNP45 affects body fat distribution and the development of atherosclerosis has not been clarified at present. Further investigations will be needed to elucidate the functional mechanism of this polymorphism.

Acknowledgements

This study was partially supported by the Second Department of Internal Medicine, Kanazawa University Hospital. We thank Mrs. Reiko Ikeda for her excellent technical assistance.

References

1) Maeda K, Okubo K, Shimomura I, Funahashi T, Matsuzawa Y, and Matsubara K: cDNA cloning and expression of a novel adipose specific collagen-like factor, apM1 (AdiPose Most abundant Gene transcript 1). Biochem Biophys Res Commun, 1996; 221:286-289
2) Scherer PE, Williams S, Fogliano M, Baldini G, and Lodish HF: A novel serum protein similar to C1q, produced exclusively in adipocytes. J Biol Chem, 1995; 270:26746-26749
3) Combs TP, Berg AH, Obici S, Scherer PE, and Rossetti L: Endogenous glucose production is inhibited by the adipose-derived protein Acrp30. J Clin Invest, 2001; 108:1875-1881
4) Yamauchi T, Kamon J, Minokoshi Y, Ito Y, Waki H, Uchida S, Yamashita S, Noda M, Kita S, Ueki K, Eto K, Akanuma Y, Froguel P, Foufelle F, Ferre P, Carling D, Kimura S, Nagai R, Kahn BB, and Kadowaki T: Adiponectin stimulates glucose utilization and fatty-acid oxidation by activating AMP-activated protein kinase. Nat Med, 2002; 8:1288-1295
5) Maeda N, Shimomura I, Kishida K, Nishizawa H, Matsuda M, Nagaretani H, Furuyama N, Kondo H, Takahashi M, Arita Y, Komuro R, Ouchi N, Kihara S, Tochino Y, Okutomi K, Horie M, Takeda S, Aoyama T, Funahashi T, and Matsuzawa Y: Diet-induced insulin resistance in mice lacking adiponectin/ACRP30. Nat Med, 2002; 8:731-737
6) Ouchi N, Kihara S, Arita Y, Nishida M, Matsuyama A, Okamoto Y, Ishigami M, Kuriyama H, Ishida K, Nishizawa H, Hotta K, Muraguchi M, Ohmoto Y, Yamashita S, Funahashi T, and Matsuzawa Y: Adipocyte-derived plasma protein, adiponectin, suppresses lipid accumulation and class A scavenger receptor expression in human monocyte-derived macrophages. Circulation, 2001; 103:1057-1063
7) Ouchi N, Kihara S, Arita Y, Okamoto Y, Maeda K, Kuriyama H, Hotta K, Nishida M, Takahashi M, Muraguchi M, Ohmoto Y, Nakamura T, Yamashita S, Funahashi T, and Matsuzawa Y: Adiponectin, an adipocyte-derived plasma protein, inhibits endothelial NF-κB signaling through a cAMP-dependent pathway. Circulation, 2000; 102:1296-1301
8) Ouchi N, Kihara S, Arita Y, Maeda K, Kuriyama H, Okamoto Y, Hotta K, Nishida M, Takahashi M, Nakamura T, Yamashita S, Funahashi T, and Matsuzawa Y: Novel modulator for endothelial adhesion molecules: adipocyte-derived plasma protein adiponectin. Circulation, 1999; 100:2473-2476
9) Fumeron F, Aubert R, Siddiq A, Betoulle D, Pean F, Hadjadj S, Tichet J, Wilpart E, Chesnier MC, Balkau B, Froguel P, and Marre M: Adiponectin gene polymorphisms and adiponectin levels are independently associated with the development of hyperglycemia during a 3-year period: the epidemiologic data on the insulin resistance syndrome prospective study. Diabetes, 2004; 53:1150-1157
10) Menzaghi C, Ercolino T, Di Paola R, Berg AH, Warram JH, Scherer PE, Trischitta V, and Doria A: A haplotype at the adiponectin locus is associated with obesity and other features of the insulin resistance syndrome. Diabetes, 2002; 51:2306-2312
11) Hara K, Bautin P, Mori Y, Tobe K, Dina C, Yasuda K, Yamauchi T, Otabe S, Okada T, Eto K, Kadowaki H, Hagura R, Akanuma Y, Yazaki Y, Nagai R, Taniyama M, Matsubara K, Yoda M, Nakano Y, Tomita M, Kimura S, Ito C, Froguel P, and Kadowaki T: Genetic variation in the gene

encoding adiponectin is associated with an increased risk of type 2 diabetes in the Japanese population. Diabetes, 2002; 51:536-540
12) Lacquemant C, Froguel P, Lobbens S, Izzo P, Dina C, and Ruiz J: The adiponectin gene SNP + 45 is associated with coronary artery disease in Type 2 (non-insulin-dependent) diabetes mellitus. Diabetic Medicine, 2004; 21:776-781
13) The Examination Committee of Criteria for 'Obesity Disease' in Japan, Japan Society for the Study of Obesity: New criteria for 'obesity disease' in Japan. Circ J, 2002; 66:987-992
14) Expert Committee on the Diagnosis and Classification of Diabetes Mellitus: Report of the Expert Committee on the Diagnosis and Classification of Diabetes Mellitus. Diabetes Care, 1997; 20:1183-1197
15) Matthews DR, Hosker JP, Rudenski AS, and Naylor BA: Homeostasis model assesment: insulin resistance and β-cell function from fasting plasma glucose and insulin concentrations in man. Diabetologia, 1985; 28:412-419
16) Yoshizumi T, Nakamura T, Yamane M, Islam AHMW, Menju M, and Yamasaki K: Abdominal fat: Standardized technique for measurement at CT. Radiology, 1999; 211:283-286
17) Nagai Y, Kitagawa K, Yamagami H, Kondo K, Hougaku H, Hori M, and Matsumoto M: Carotid artery intima-media thickness and plaque score for the risk assessment of stroke subtypes. Ultrasound Med Biol, 2002; 28:1239-1243
18) Stumvoll M, Tschritter O, Fritsche A, Staiger H, Renn W, Weisser M, Machicao F, and Haring H: Association of the T-G polymorphism in adiponectin (exon 2) with obesity and insulin sensitivity: interaction with family history of type 2 diabetes. Diabetes, 2002; 51:37-41
19) Kondo H, Shimomura I, Matsukawa Y, Kumada M, Takahashi M, Matsuda M, Ouchi N, Kihara S, Kawamoto T, Sumitsuji S, Funahashi T, and Matsuzawa Y: Association of adiponectin mutation with type 2 diabetes: a candidate gene for the insulin resistance syndrome. Diabetes, 2002; 51:2325-2328
20) Ukkola O, Ravussin E, Jacobson P, and Bouchard C: Mutations in the adiponectin gene in lean and obese subjects from the Swedish obese subjects cohort. Metabolism, 2003; 52:881-884
21) Bouatia-Naji N, Meyre D, Lobbens S, Seron K, Fumeron F, Balkan B, Heude B, Jouret B, Scherer P, Dina C, Weill J, and Froguel P: ACDC/Adiponectin polymorphism are associated with severe childhood and adult obesity. Diabetes, 2006; 55:545-549
22) Murase Y, Asano A, Kobayashi J, Yamaaki N, and Mabuchi H: Impact of adiposity on carotid atherosclerosis in Japanese males with metabolic syndrome. J Intern Med, 2005; 257:311-312
23) Butte NF, Hopkinson JM, Wong WW, Smith EO, and Ellis KJ: Body composition during the first 2 years of life: an updated reference. Pediatr Res, 2000; 47:578-585
24) Taylor RW, Jones IE, Williams SM, and Goulding A: Body fat percentages measured by dual-energy X-ray absorptiometry corresponding to recently recommended body mass index cutoffs for overweight and obesity in child and adolescents aged 3-18 y. Am J Clin Nutr, 2002; 76:1416-1421
25) Marin P and Bjorntorp: Endocrine-metabolic patterns and adipose tissue distribution. Horm Res, 1993; 39:81-85
26) Rosenbaum M and Leibel RL: Role of gonadal steroids in the sexual dimorphisms in body composition and circulating concentrations of leptin. J Clin Endocrinol Metab, 1999; 84:1784-1789
27) Cooke PS and Naaz A: Role of estrogens in adipocyte development and function. Exp Biol Med, 2004; 229:1127-1135
28) Clegg D, Brown L, Woods S, and Benoit S; Gonadal hormones determine sensitivity to central leptin and insulin. Diabetes, 2006; 55:978-987
29) Simoncini T, Maffei S, and Basta G: Estrogens and glucocorticoids inhibit endotherial vascular cell adhesion molecule-1 expression by different transcriptional mechanisms. Circ Res, 2000; 87:19-25
30) Hsu SM, Chen YC, and Jiang MC: 17β-estradiol inhibits tumor necrosis factor-α-induced nuclear factor-κB activation by increasing nuclear factor-κB p105 level in MCF-7 breast cancer cells. Biochem Biophys Res Commun, 2000; 279:47-52
31) Takahashi M, Arita Y, Yamagata K, Matsukawa Y, Okutomi K, Horie M, Shimomura I, Hotta K, Kuriyama H, Kihara S, Nakamura T, Yamashita S, Funahashi T, and Matsuzawa Y: Genomic structure and mutations in adipose-specific gene, adiponectin. Int J Obes Relat Metab Disord, 2000; 24:861-868
32) Fu Y, Luo N, Klein R, and Garvey W: Adiponectin promotes adipocyte differentiation, insulin sensitivity, and lipid accumulation. Journal of Lipid Research, 2005; 46:1369-1379
33) Pajvani UB, Du X, Combs TP, Berg AH, Rajala MW, Schulthess T, Engel J, Brownlee M, and Scherer PE: Structure-function studies of the adipocyte-secreted hormone Acrp30/adiponectin: implications for metabolic regulation and bioactivity. J Biol Chem, 2003; 278:9073-9085
34) Pajvani UB, Hawkins M, Combs TP, Rajala MW, Doebber T, Berger JP, Wagner JA, Wu M, Knopps A, Xiang AH, Utzschneider KM, Kahn SE, Olefsky JM, Buchanan TA, and Scherer PE: Complex distribution, not absolute amount of adiponectin, correlate with thiazolidinedione-mediated improvement in insulin sensitivity. J Biol Chem, 2004; 279:12152-12162
35) Lara-Castro C, Luo N, Wallace P, Klein R, and Garvey W: Adiponectin multimeric complexes and the metabolic syndrome trait cluster. Diabetes, 2006; 55:249-259

High Frequency of a Retinoid X Receptor γ Gene Variant in Familial Combined Hyperlipidemia That Associates With Atherogenic Dyslipidemia

Atsushi Nohara, Masa-aki Kawashiri, Thierry Claudel, Mihoko Mizuno, Masayuki Tsuchida, Mutsuko Takata, Shoji Katsuda, Kenji Miwa, Akihiro Inazu, Folkert Kuipers, Junji Kobayashi, Junji Koizumi, Masakazu Yamagishi, Hiroshi Mabuchi

Objective—The genetic background of familial combined hyperlipidemia (FCHL) has not been fully clarified. Because several nuclear receptors play pivotal roles in lipid metabolism, we tested the hypothesis that genetic variants of nuclear receptors contribute to FCHL.

Methods and Results—We screened all the coding regions of the PPARα, PPARγ2, PPARδ, FXR, LXRα, and RXRγ genes in 180 hyperlipidemic patients including 60 FCHL probands. Clinical characteristics of the identified variants were evaluated in other 175 patients suspected of coronary disease. We identified PPARα Asp140Asn and Gly395Glu, PPARγ2 Pro12Ala, RXRγ Gly14Ser, and FXR −1g−>t variants. Only RXRγ Ser14 was more frequent in FCHL (15%, $P<0.05$) than in other primary hyperlipidemia (4%) and in controls (5%). Among patients suspected of coronary disease, we identified 9 RXRγ Ser14 carriers, who showed increased triglycerides (1.62±0.82 versus 1.91±0.42 [mean±SD] mmol/L, $P<0.05$), decreased HDL-cholesterol (1.32±0.41 versus 1.04±0.26, $P<0.05$), and decreased post-heparin plasma lipoprotein lipase protein levels (222±85 versus 149±38 ng/mL, $P<0.01$). In vitro, RXRγ Ser14 showed significantly stronger repression of the lipoprotein lipase promoter than RXRγ Gly14.

Conclusion—These findings suggest that RXRγ contributes to the genetic background of FCHL. (***Arterioscler Thromb Vasc Biol.* 2007;27:923-928.**)

Key Words: apolipoproteins ■ gene mutations ■ lipoprotein lipase ■ familial combined hyperlipidemia ■ nuclear receptors

Familial combined hyperlipidemia (FCHL) is the most common form of inherited hyperlipidemia. FCHL shows strong genetic susceptibility resembling an autosomal dominant disease,[1–3] but most of the underlying causal mechanisms remain to be elucidated. Lipoprotein lipase (LPL) has been implicated as one of the genes that modify the lipid phenotype in FCHL.[4,5] "Intra-individual variability" of the lipoprotein phenotype is often included as a criterion in diagnosis.[6] However, a recent prospective study of FCHL families suggests that this variability may even include normolipidemic periods in affected subjects.[7] This feature indicates that FCHL could be a "disease of regulation" rather than a genetic defect in certain peripheral components of lipid metabolism.

Nuclear receptors are transcription factors that can be activated by specific ligands. Recent studies have shown that nuclear receptors, especially retinoid X receptor (RXR) and its heterodimerization partners,[8] play important roles in maintenance of lipid homeostasis on their activation by a variety of ligands derived from dietary cholesterol and fatty acids.[9] The peroxisome proliferator-activated receptors (PPARs) family, the oxysterol sensor liver X receptor (LXR), and the bile acid sensor farnesoid X receptor (FXR) are all involved in control of plasma lipid concentrations.[10] Thus, we tested the hypothesis that variants of these nuclear receptors, ie, PPARα, PPARγ2, PPARδ, LXRα, FXR, and RXRγ, could constitute part of the genetic background of atherogenic dyslipidemia, particularly of FCHL.

Methods

Subjects

The study design consists of 2 parts. First, we screened for frequent variants in the nuclear receptor candidate genes among 180 patients with primary hyperlipidemia, including 60 unrelated patients with FCHL (clinical characteristics are presented in supplemental Table I, available online at http://atvb.ahajounals.org). Patients with familial

Original received August 28 2006; final version accepted January 6, 2007.

From the Departments of Lipidology (A.N., M.M., J. Kobayashi, H.M.) and Cardiovascular Medicine (M.K., M. Tsuchida, M. Takata, S.K., K.M., M.Y.), Graduate School of Medical Science, Kanazawa University, Japan; Center for Liver, Digestive, and Metabolic Diseases, Laboratory of Pediatrics (T.C., F.K.), University Medical Center Groningen, Groningen, the Netherlands; School of Health Sciences, Faculty of Medicine (A.I.), and Department of General Medicine (J. Koizumi), Kanazawa University Hospital, Japan.

Correspondence to Atsushi Nohara, Department of Lipidology, Graduate School of Medical Science, Kanazawa University, Takara-machi 13-1, Kanazawa 920-8641, Japan. E-mail a-nohara@med.kanazawa-u.ac.jp

Arterioscler Thromb Vasc Biol. is available at http://www.atvbaha.org DOI: 10.1161/01.ATV.0000258945.76141.8a

hypercholesterolemia and secondary hyperlipidemia were excluded. Diagnosis of FCHL was based on the fulfillment of all of the following three criteria: (1) Phenotype IIb, IIa, or IV hyperlipidemia according to the Fredrickson classification; (2) Presence of phenotype IIb, IIa, or IV hyperlipidemia in a first-degree relative and at least one family member with phenotype IIb; (3) Exclusion of familial hypercholesterolemia. Two hundred ninety-eight anonymous samples from healthy males were used as controls for frequency analysis of identified mutations. All blood samples in this study were obtained after an overnight fast.

Second, we evaluated the clinical impact of potentially relevant variants in another 175 patients who were suspected of having coronary artery disease based on any of the following reasons: ECG abnormalities, cumulative coronary risk factors, and/or chest symptoms. The group included 105 patients who had undergone coronary angiography. Patients with familial hypercholesterolemia were excluded because of their clear genetic background for hyperlipidemia. The extent and severity of atherosclerotic changes in coronary angiography were assessed by assigning scores to each of the 15 segments, according to the classification of the American Heart Association Grading Committee. The coronary stenosis index (CSI) was defined as the sum of the following scores[11]: A normal coronary angiogram was graded 0, stenosis of less than 25% was graded 1, 25% to 50% stenosis was graded 2, 50% to 75% stenosis was graded 3, and more than 75% stenosis was graded 4. CSI is a useful index for evaluating mild-moderate coronary atherosclerotic changes.

All the subjects and controls enrolled were inhabitants of the Hokuriku district of Japan. Written informed consent was obtained from each of the subjects. The study protocol was approved by the ethics committee of the Graduate School of Medical Science, Kanazawa University.

Laboratory Analyses

Total cholesterol (TC), triglycerides (TG), high-density lipoprotein (HDL)-cholesterol, apolipoproteins, glucose, and thyroid hormones were measured according to standard clinical laboratory techniques. HDL-cholesterol fractions were obtained by dextran sulfate-magnesium chloride precipitation and assayed using a commercial kit (Daiichi, Tokyo, Japan).[12] Separation of lipoproteins by ultracentrifugation was performed as described by Havel et al.[13] Plasma remnant-like particle (RLP)-cholesterol was determined by immunoabsorption using the commercial RLP-C JIMRO kit.[14] Plasma cholesteryl ester transfer protein (CETP) concentrations were determined by enzyme-linked immunosorbent assay using the monoclonal antibody TP2 and a rabbit polyclonal antibody raised against recombinant human CETP.[15] For LPL assessment, blood samples were obtained 10 minutes after an intravenous injection of 30 IU heparin/kg body weight. LPL activity was measured using radiolabeled triolein emulsion after hepatic lipase (HL) inhibition by SDS as previously described.[16] LPL mass was measured by sandwich enzyme-linked immunosorbent assay (ELISA) using specific monoclonal antibody against LPL (Daiichi Pure Chemicals Co Ltd, Tokyo, Japan).[17]

Genetic Analyses of Candidate Genes

Genomic DNA was isolated from peripheral white blood cells using standard phenol-chloroform extraction techniques. We screened all the coding regions of PPARα (NM_032644), PPARδ (NM_006238), PPARγ2 (NM_015869), LXRα (NM_005693), FXR (NM_005123), and RXRγ (NM_006917) genes with flanking exon-intron boundaries by polymerase chain reaction (PCR)-denaturing gradient gel electrophoresis (DGGE) using the DCode system (Bio-Rad), which is highly accurate in detecting changes in nucleic acids.[18] The structural organization and nucleotide sequences of these genes were retrieved from the gene database of NCBI. Lists of all GC-clamped primers used in DGGE analysis are available online (supplemental Table II). Samples with a variant detected by DGGE analysis were directly sequenced on an ABI310 analyzer (Applied Biosystems). PCR-restriction-fragment-length polymorphisms analysis on the RXRγ Ser14 variant was performed with the primers 5′-AGCCGAGAGAGGCGGTAATA-3′ (forward) and 5′-TACAGGTCCACGCAGTGAAG-3′ (reverse) in patients suspected of coronary artery disease. Digestion with *Alu*I resulted in a 76-bp fragment for Ser allele and a 120-bp fragment for Gly allele.

Cell Culture and Transfection Assays

Cos7 cells were grown in DMEM supplemented with 10% FCS, penicillin/streptomycin, sodium pyruvate, glutamine, and nonessential amino acids (Gibco BRL, Invitrogen). The medium was changed every 48 hours. Cos7 cells were transfected using FuGENE 6 reagent (Roche): 150 ng of the indicated LPL firefly luciferase reporter plasmid (a generous gift of Dr B. Staels, Institut Pasteur de Lille, France), that contains the proximal 466-bp of the human LPL promoter in front of the ATG cloned into the *Hind*III site of the pGL3 plasmid, was cotransfected with or without 100 ng of the human RXRγ expressing vector (a generous gift of Dr W. Lamph, Ligand Pharmaceuticals Inc, San Diego, Calif). After an overnight incubation, cells were incubated with medium containing 10% FCS with or without the retinoid LGD1069, (1 μmol/L, Sigma) and luciferase activity was assayed 48 hours later using an Orion luminometer (Berthold). Transfection studies were performed at least 3 times in triplicate. Transfection efficiency was monitored by cotransfection of 150 ng of a SV40-driven β-galactosidase expression plasmid. A positive RXRE TKpGL3 construct was made by cloning 3 copies of the direct repeat AGGTCA spaced by 5 nucleotides in the TKpGL3 plasmid.

Plasmid Site-Directed Mutagenesis

Nucleotide substitution was introduced in the plasmid expressing human RXRγ using the QuikChange Site-Directed Mutagenesis Kit (Stratagene, The Netherlands) and the primer 5′-CATGAAGTTTCCCGCAAGCTATGGAGGCTCCCCTGG C-3′ in which the nucleotide in bold indicates the mutation.

Statistical Analysis

The frequency distribution of genotypes was compared using standard χ^2 tests. Student *t* test was used for normally distributed parameters and the Kruskal–Wallis test was used for non-normally distributed parameters: triglycerides levels, LPL levels, and CSI. JMP 5.1.2 software (SAS Institute Inc) was used for statistical calculation.

Results

Identified Variants in Nuclear Receptor Genes

With PCR-DGGE analysis, we identified 4 variants with amino acid changes, ie, Asp140Asn and Gly395Glu in the PPARα gene, Pro12Ala in the PPARγ2 gene, Gly14Ser in the

TABLE 1. Frequencies of Nuclear Receptor Genes Variants Identified in This Study

	FCHL n=60	Other Hyperlipidemia n=120	General Population n=298	*P* Value
PPARαGly395Glu				
Glu395	3 (5%)	1 (0.8%)	6 (2%)	ns
PPARαAsp140Asn				
Asn140	2 (3%)	1 (0.8%)	2 (0.6%)	ns
PPARγ2Pro12Ala				
Ala12	5 (8%)	10 (8%)	20 (7%)	ns
FXR −1g−>t				
−1g/t	19 (32%)	34 (28%)	108 (36%)	ns
−1t/t	2 (3%)	6 (5%)	27 (9%)	ns
RXRγGly14Ser				
Ser14	9 (15%)	5 (4%)	15 (5%)	0.03

TABLE 2. Clinical Characteristics of Patients With RXRγ Variant

	RXRγ Gly14Ser		
	Gly/Gly	Gly/Ser	*P* Value
Number (M/F)	166 (78/88)	9 (5/4)	
Age, y	58±15	58±7	ns
BMI, kg/m^2	23.4±5	23.9±2	ns
Smoking, %	36	33	ns
Total cholesterol, mmol/L	5.98±1.4	5.96±1.55	ns
Triglycerides, mmol/L	1.62±0.82	1.91±0.42	*P*<0.05
HDL cholesterol, mmol/L	1.32±0.41	1.04±0.26	*P*<0.05
LDL cholesterol, mmol/L	3.94±1.27	4.07±1.45	ns
HDL2 cholesterol, mmol/L	0.78±0.28	0.54±0.10	*P*<0.05
HDL3 cholesterol, mmol/L	0.44±0.10	0.39±0.08	ns
ApoA-I, g/L	1.38±0.31	1.18±0.18	ns
ApoA-II, g/L	0.32±0.06	0.28±0.05	*P*<0.05
ApoB, g/L	1.31±0.38	1.35±0.31	ns
ApoC-II, g/L	0.06±0.02	0.05±0.02	ns
ApoC-III, g/L	0.11±0.05	0.10±0.03	ns
ApoE, g/L	0.06±0.02	0.05±0.01	ns
RLP cholesterol, mmol/L	0.15±0.10	0.21±0.10	*P*<0.01
CETP, mg/L	2.52±0.82	2.48±0.73	ns
Intraindividual lipoprotein phenotype variability, %	27	88	*P*<0.01
Fasting glucose, mmol/L	5.72±1.39	5.33±0.72	ns
HbA1c, %	5.6±1.0	5.8±1.0	ns
Fasting insulin, pmol/L	70.8±90.3	52.1±1.0	ns
HOMA-IR	2.28±2.1	2.19±1.7	ns
Diabetes, %	28	33	ns
HL activity, U/L	0.24±0.09	0.26±0.07	ns
LPL activiy, U/L	0.11±0.06	0.08±0.03	*P*<0.05
LPL mass, ng/mL	222±85	149±38	*P*<0.01
FT3, pmol/L	0.42±0.01	0.044±0.01	ns
FT4, pmol/L	15.2±5.15	13.3±2.57	ns
TSH, μU/mL	2.31±2.8	2.53±0.9	ns
Number (M/F)	100 (50/50)	5 (4/1)	
CSI	12.3±10	21.4±6	*P*<0.05
			mean±SD

BMI indicates body mass index; HOMA-IR, homeostasis model assessment; FT3, free triiodothyronine; FT4, free thyroxine; TSH, thyroid stimulating hormone.

RXRγ gene, and 1 nucleotide substitution in a flanking coding region, ie, FXR −1g−>t variant. The PPARγ2 Pro12Ala polymorphism has already been well-described,[19] whereas the others represent novel variants identified in this study. In humans, variants in the RXRγ gene have been associated with elevated triglyceride levels in familial type 2 diabetes, but none of these variants showed an altered coding sequence.[20] Therefore, this is the first description of a RXRγ variant with an amino acid substitution. In the PPARα gene, the Leu162Val variant has been reported in Western countries,[21] but this variant was not identified in this study. We also identified some silent nucleotide substitutions, ie, 891C−>G (rs13306747) and 1431C−>T (rs1724155) in the PPARγ2 gene, 1233C−>T (rs9658166) in the PPARδ gene, and 1134A−>G (rs1131379) in the LXRα gene. We did not identify variants with amino acid changes in the PPARδ and LXRα genes. We further investigated the variants with amino acid substitutions and the −1g−>t FXR variant, because of the likelihood that these induced altered physiological function.

Higher Frequency of RXRγ Variant in FCHL

We evaluated the frequencies of the 5 identified polymorphisms in subjects with FCHL, subjects with other forms of primary hyperlipidemia and in the general population (Table 1). Only the RXRγ Ser14 variant was found to be significantly more frequent in FCHL patients (15%) compared with that in other forms of primary hyperlipidemia (4%) or the general population (5%).

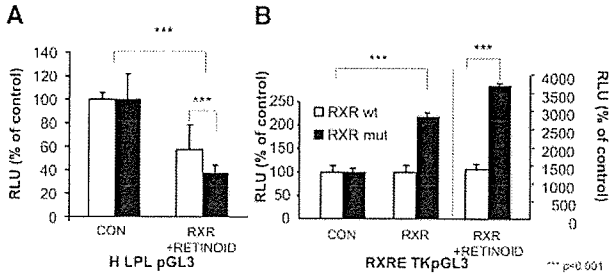

A, Cos7 cells were cotransfected with RXRγ wild-type or the Ser14 variant and activated with retinoid in presence of the LPL promoter. B, Cos7 cells were cotransfected with RXRγ wild-type or the Ser14 variant and activated with retinoid in presence of a positive RXRE cloned in the TKpGL3 plasmid.

Atherogenic Plasma Lipids Profiles and Coronary Atherosclerosis Associated With the RXRγ Ser14 Variant

To establish the impact of the identified RXRγ variant on metabolic parameters and on coronary atherosclerosis, we evaluated anthropometric parameters and laboratory data from 175 patients suspected of coronary disease. The RXRγ Ser14 variant was identified in 9 patients, all of whom were heterozygotes. Eight of the RXRγ Ser14 carriers had hyperlipidemia, while the remaining 1 demonstrated an isolated low HDL cholesterol level. Clinical characteristics of patients with or without the RXRγ Ser14 allele are shown in Table 2. There was no difference in age or body mass index between the two groups. In their lipid profiles, RXRγ Ser14 carriers had higher TG, lower HDL cholesterol especially in the HDL2 subfraction, and lower apolipoprotein A-II levels. There was no difference in CETP protein levels between the groups. Furthermore, we found that the RLP cholesterol level was significantly higher in the RXRγ Ser14 carriers than in the wild-type. Subjects with this variant also showed significantly lower LPL activities and protein levels in post-heparin plasma. Separation of lipoproteins demonstrated that the Ser14 carriers had higher TG levels in very low-density lipoprotein (VLDL) and low-density lipoprotein (LDL) fractions, higher cholesterol levels in VLDL, and lower cholesterol levels in HDL (supplemental Table III).

Two RXRγ Ser14 carriers were diagnosed as FCHL (22%), and 2 additional carriers were suspected of FCHL with hyperlipidemic siblings without information on first-degree relatives. Among non-carriers, 22 of 166 patients were diagnosed as FCHL (13%). One hundred twenty-five patients suspected of coronary disease showed hyperlipidemia and the intraindividual variability of lipoprotein phenotype was significantly more frequent in RXRγ Ser14 carriers (7 of 8 hyperlipidemic patients; 88%) than in wild-type (32 of 117 hyperlipidemic patients; 27%, Table 2).

There was no significant difference in the thyroid hormone levels between the two groups.

Four males and 1 female were identified as RXRγ variant carriers among 105 patients who underwent coronary angiography. The carriers of RXRγ Ser14 demonstrated significantly higher CSI than those with the wild-type (Table 2).

RXRγ Variant Represses More Efficiently the LPL Promoter Activity

Because RXRγ Ser14 carriers showed significantly lower LPL activities and protein levels in post-heparin plasma, we hypothesized that activated-RXRγ downregulates LPL gene expression by a transcriptional mechanism and that RXRγ variant is more effective in repressing the LPL promoter activity. Therefore, transfection assays were performed using the LPL promoter cotransfected with either wild-type RXRγ or the variant (Figure). Interestingly, RXRγ Gly14 significantly repressed (−40%) the LPL promoter activity, whereas the RXRγ Ser14 repressed even more strongly (−60%, $P<0.001$, Figure A). Moreover, the RXRγSer14 was a more potent activator of a positive RXRE cloned in front of a TKpGL3 plasmid (note the different scales in Figure B). Taken together, our results indicate that RXRγ downregulates human LPL gene expression, at least partially by a transcriptional mechanism, and that the newly identified RXRγ variant is a more potent repressor than the wild-type in this respect, as well as a more potent transactivator of a positive RXR response element.

Gain of Function Variant of PPARα and Increased LDL-C Levels

The carriers of the PPARα variant Gly395Glu tended to have higher frequency in the FCHL population, although not statistically significant. Four subjects were identified as PPARα Glu395 carriers in the coronary artery disease-suspected group and showed significantly higher LDL-cholesterol levels (supplemental Table IV). On in vitro functional analysis, Glu395 showed a moderately but significantly increased transcriptional activity compared with wild-type PPARα (supplemental Figure I, available online at http://atvb.ahajournals.org). The previously described Leu162Val variant of the PPARα gene has been shown to give gain of function in in vitro,[24] has been associated with raised LDL-cholesterol levels.[21,22] Our results appear to be in accordance with these previous reports.

Discussion

The main findings of the present study are the following: (1) identification of novel polymorphisms in plasma lipid levels-associated nuclear receptor genes, (2) a higher frequency of the RXRγ gene variant Gly14Ser in subjects with FCHL, (3) RXRγ Ser14 variant carriers showed more atherogenic dyslipidemia associated with coronary atherosclerosis, (4) the RXRγ variant showed a stronger response to its ligand in repression of the LPL promoter than the wild-type RXRγ.

RXRs are major heterodimerization partners of nuclear receptors such as PPARs, LXRs, and FXR. Three RXR isotypes have been identified: RXRα, RXRβ, and RXRγ. Synthetic RXR ligands induce hypertriglyceridemia through decreased clearance of VLDL by LPL-dependent pathways,[23,24] except in 1 study.[25] In contrast to the embryonic lethality observed in RXRα- and RXRβ-deficient mice, RXRγ-deficient mice develop apparently normal.[26] Yet, RXRγ-deficient mice showed reduced fasting plasma TG levels and increased skeletal muscle LPL activity when fed a high fat diet.[27] The human RXRγ gene is located on chro-

mosome 1q21-q23, ie, the so-called "FCHL locus",[28] and both linkage analysis and a twin study have indicated that the RXRγ gene is linked with dyslipidemia in Chinese and German families.[29,30]

To our knowledge, there are only few data concerning the physiological roles and targets of RXRγ in humans. The RXRγ gene is mainly expressed in skeletal muscles, central nervous system, skin, intestine, and lung. In the present study, LPL protein mass and activity were significantly decreased in RXRγ variant carriers. Because LPL is mainly expressed in adipose tissues and in skeletal muscles, we assume that this is attributable to the fact that the presence of the RXRγ variant affects LPL expression in skeletal muscles. RXRγ mRNA is detectable in adipose tissue only at a low level,[31] but it has been reported that RXRγ could replace RXRα in heterodimerization with PPARγ in adipose tissue.[32] Therefore, there is a possibility that RXRγ variant expression in adipose tissue contributes to the changes in LPL.

It has been reported that RXRγ-deficient mice show a 17% increase in serum thyroid hormone (T4) and a 20% increase in thyroid-stimulating hormone (TSH) levels.[33] In the present study, thyroid hormone levels did not appear to differ sufficiently between variant carriers and non-carriers to explain the differences observed in lipid levels.

It has been shown that low LPL levels contribute to disorders associated with TG-rich lipoprotein catabolism with low HDL, especially in HDL2,[34,35] and are associated with increased risk for future coronary disease.[36] Thus, the low LPL could well contribute to the increase in TG and the decrease in HDL-cholesterol levels in subjects with the RXRγ variant.

We assessed the functional consequence of the RXRγ Ser14 variant in vitro. The activation function-1 (AF-1) domain of RXRγ is located between amino acids 1 and 103, and is required for optimal ligand-dependent transactivation of RXR response element.[37] Fourteen amino acids are located within the AF-1 domain and are conserved among humans, mice, and chickens. In a transfection assay, RXRγ Ser14 repressed LPL promoter activity more strongly than the wild-type RXRγ. In addition, the Ser14 variant was a more potent inducer of a positive RXR response element. Therefore, we speculate that the Ser14 variant induces a better recruitment and/or stabilization of RXR cofactors. Further studies will be required to understand the precise molecular mechanism(s) involved in the LPL regulation by RXRγ Ser14.

Within the so-called FCHL locus, on chromosome 1q21-q23, several genes have been reported to be associated with the FCHL phenotype[28,30,38] and with type 2 diabetes.[39] First, the thioredoxin interacting protein gene was shown to be associated with combined hyperlipidemia in mice, but no disease-causing mutation has been found in humans so far.[40,41] Currently upstream stimulatory factor 1 (USF1) is considered the most promising candidate gene of FCHL.[42] In the USF1 gene, no amino acid substitution has been identified in the coding regions, but single nucleotide polymorphisms in the 3′untranslated region and in intron 7 have been reported to be associated with FCHL, metabolic syndrome, or type 2 diabetes mellitus quite reproducibly.[43–45] However, populations did not show any such association have also been reported.[46–48] These reports emphasize the complexity of phenotypic expression in multi-factorial diseases such as FCHL. RXRγ had been reported to show an association with TG and cholesterol levels on linkage analysis,[29,30] and we identified novel RXRγ variant that associated with atherogenic dyslipidemia. However, the changes in lipid levels attributable to the RXRγ variant alone were not sufficient to cause FCHL. Thus, we suggest the RXRγ gene variant to be a strong modifier rather than a causative gene in development of the FCHL phenotype.

In conclusion, the present study suggests that a variant of RXRγ gene contributes to genetic dyslipidemia, including FCHL, based on the increased frequency of this variant in FCHL, its association with an atherogenic lipid profile, and initial functional studies.

Acknowledgments

The authors thank Sachio Yamamoto for technical assistance. Drs William W. Lamph and Bart Staels are kindly acknowledged for the generous gift of plasmids.

Sources of Funding

This work has been supported by a scientific research grant from the Ministry of Education, Science, and Culture of Japan (No.17790603) and ONO Medical Research Foundation. Thierry Claudel was supported by Grant 2002B017 from the Netherlands Heart Foundation.

Disclosures

None.

References

1. Goldstein JL, Schrott HG, Hazzard WR, Bierman EL, Motulsky AG. Hyperlipidemia in coronary heart disease. II. Genetic analysis of lipid levels in 176 families and delineation of a new inherited disorder, combined hyperlipidemia. *J Clin Invest.* 1973;52:1544–1568.
2. Rose HG, Kranz P, Weinstock M, Juliano J, Haft JI. Inheritance of combined hyperlipoproteinemia: evidence for a new lipoprotein phenotype. *Am J Med.* 1973;54:148–160.
3. Nikkila EA, Aro A. Family study of serum lipids and lipoproteins in coronary heart-disease. *Lancet.* 1973;1:954–959.
4. Hoffer MJ, Bredie SJ, Snieder H, Reymer PW, Demacker PN, Havekes LM, Boomsma DI, Stalenhoef AF, Frants RR, Kastelein JJ. Gender-related association between the -93T−>G/D9N haplotype of the lipoprotein lipase gene and elevated lipid levels in familial combined hyperlipidemia. *Atherosclerosis.* 1998;138:91–99.
5. Hoffer MJ, Bredie SJ, Boomsma DI, Reymer PW, Kastelein JJ, de Knijff P, Demacker PN, Stalenhoef AF, Havekes LM, Frants RR. The lipoprotein lipase (Asn291−>Ser) mutation is associated with elevated lipid levels in families with familial combined hyperlipidaemia. *Atherosclerosis.* 1996;119:159–167.
6. Gaddi A, Galetti C, Pauciullo P, Arca M. Familial combined hyperlipoproteinemia: experts panel position on diagnostic criteria for clinical practice. Committee of experts of the Atherosclerosis and Dysmetabolic Disorders Study Group. *Nutr Metab Cardiovasc Dis.* 1999;9:304–311.
7. Veerkamp MJ, de Graaf J, Bredie SJ, Hendriks JC, Demacker PN, Stalenhoef AF. Diagnosis of familial combined hyperlipidemia based on lipid phenotype expression in 32 families: results of a 5-year follow-up study. *Arterioscler Thromb Vasc Biol.* 2002;22:274–282.
8. Mangelsdorf DJ, Evans RM. The RXR heterodimers and orphan receptors. *Cell.* 1995;83:841–850.
9. Shulman AI, Mangelsdorf DJ. Retinoid x receptor heterodimers in the metabolic syndrome. *N Engl J Med.* 2005;353:604–615.
10. Claudel T, Staels B, Kuipers F. The Farnesoid X receptor: a molecular link between bile acid and lipid and glucose metabolism. *Arterioscler Thromb Vasc Biol.* 2005;25:2020–2030.

11. Mabuchi H, Koizumi J, Shimizu M, Takeda R. Development of coronary heart disease in familial hypercholesterolemia. *Circulation.* 1989;79: 225–232.
12. Talameh Y, Wei R, Naito H. Measurement of total HDL, HDL2, and HDL3 by dextran sulfate-MgCl2 precipitation technique in human serum. *Clin Chim Acta.* 1986;158:33–41.
13. Havel RJ, Eder HA, Bragdon JH. The distribution and chemical composition of ultracentrifugally separated lipoproteins in human serum. *J Clin Invest.* 1955;34:1345–1353.
14. Nakajima K, Saito T, Tamura A, Suzuki M, Nakano T, Adachi M. Tanaka A, Tada N, Nakamura H, Campos E, et al. Cholesterol in remnant-like lipoproteins in human serum using monoclonal anti apo B-100 and anti apo A-I immunoaffinity mixed gels. *Clin Chim Acta.* 1993;223:53–71.
15. Kiyohara T, Kiriyama R, Zamma S, Inazu A, Koizumi J, Mabuchi H, Chichibu K. Enzyme immunoassay for cholesteryl ester transfer protein in human serum. *Clin Chim Acta.* 1998;271:109–118.
16. Baginsky ML, Brown WV. A new method for the measurement of lipoprotein lipase in postheparin plasma using sodium dodecyl sulfate for the inactivation of hepatic triglyceride lipase. *J Lipid Res.* 1979;20:548–556.
17. Kobayashi J, Hashimoto H, Fukamachi I, Tashiro J, Shirai K, Saito Y, Yoshida S. Lipoprotein lipase mass and activity in severe hypertriglyceridemia. *Clin Chim Acta.* 1993;216:113–123.
18. Grompe M. The rapid detection of unknown mutations in nucleic acids. *Nat Genet.* 1993;5:111–117.
19. Stumvoll M, Haring H. The peroxisome proliferator-activated receptor-gamma2 Pro12Ala polymorphism. *Diabetes.* 2002;51:2341–2347.
20. Wang H, Chu W, Hemphill C, Hasstedt SJ, Elbein SC. Mutation screening and association of human retinoid X receptor gamma variation with lipid levels in familial type 2 diabetes. *Mol Genet Metab.* 2002;76: 14–22.
21. Flavell DM, Pineda Torra I, Jamshidi Y, Evans D, Diamond JR, Elkeles RS, Bujac SR, Miller G, Talmud PJ, Staels B, Humphries SE. Variation in the PPARalpha gene is associated with altered function in vitro and plasma lipid concentrations in Type II diabetic subjects. *Diabetologia.* 2000;43:673–680.
22. Tai ES, Demissie S, Cupples LA, Corella D, Wilson PW, Schaefer EJ, Ordovas JM. Association between the PPARA L162V polymorphism and plasma lipid levels: the Framingham Offspring Study. *Arterioscler Thromb Vasc Biol.* 2002;22:805–810.
23. Vahlquist C, Lithell H, Michaelsson G, Selinus I, Vahlquist A, Vessby B. Plasma fat elimination tissue lipoprotein lipase activity and plasma fatty acid composition during sequential treatment with etretinate and isotretinoin. *Acta Derm Venereol.* 1987;67:139–144.
24. Davies PJ, Berry SA, Shipley GL, Eckel RH, Hennuyer N, Crombie DL, Ogilvie KM, Peinado-Onsurbe J, Fievet C, Leibowitz MD, Heyman RA, Auwerx J. Metabolic effects of rexinoids: tissue-specific regulation of lipoprotein lipase activity. *Mol Pharmacol.* 2001;59:170–176.
25. Mukherjee R, Davies PJ, Crombie DL, Bischoff ED, Cesario RM, Jow L, Hamann LG, Boehm MF, Mondon CE, Nadzan AM, Paterniti JR Jr, Heyman RA. Sensitization of diabetic and obese mice to insulin by retinoid X receptor agonists. *Nature.* 1997;386:407–410.
26. Krezel W, Dupe V, Mark M, Dierich A, Kastner P, Chambon P. RXR gamma null mice are apparently normal and compound RXR alpha +/-/RXR beta -/-/RXR gamma -/- mutant mice are viable. *Proc Natl Acad Sci U S A.* 1996;93:9010–9014.
27. Haugen BR, Jensen DR, Sharma V, Pulawa LK, Hays WR, Krezel W, Chambon P, Eckel RH. Retinoid X receptor gamma-deficient mice have increased skeletal muscle lipoprotein lipase activity and less weight gain when fed a high-fat diet. *Endocrinology.* 2004;145:3679–3685.
28. Pajukanta P, Nuotio I, Terwilliger JD, Porkka KV, Ylitalo K, Pihlajamaki J, Suomalainen AJ, Syvanen AC, Lehtimaki T, Viikari JS, Laakso M, Taskinen MR, Ehnholm C, Peltonen L. Linkage of familial combined hyperlipidaemia to chromosome 1q21–q23. *Nat Genet.* 1998;18: 369–373.
29. Knoblauch H, Busjahn A, Muller-Myhsok B, Faulhaber HD, Schuster H, Uhlmann R, Luft FC. Peroxisome proliferator-activated receptor gamma gene locus is related to body mass index and lipid values in healthy nonobese subjects. *Arterioscler Thromb Vasc Biol.* 1999;19:2940–2944.
30. Pei W, Baron H, Muller-Myhsok B, Knoblauch H, Al-Yahyaee SA, Hui R, Wu X, Liu L, Busjahn A, Luft FC, Schuster H. Support for linkage of familial combined hyperlipidemia to chromosome 1q21–q23 in Chinese and German families. *Clin Genet.* 2000;57:29–34.
31. Kamei Y, Kawada T, Kazuki R, Sugimoto E. Retinoic acid receptor gamma 2 gene expression is up-regulated by retinoic acid in 3T3–L1 preadipocytes. *Biochem J.* 1993;293(Pt 3):807–812.
32. Metzger D, Imai T, Jiang M, Takukawa R, Desvergne B, Wahli W, Chambon P. Functional role of RXRs and PPARgamma in mature adipocytes. *Prostaglandins Leukot Essent Fatty Acids.* 2005;73:51–58.
33. Brown NS, Smart A, Sharma V, Brinkmeier ML, Greenlee L, Camper SA, Jensen DR, Eckel RH, Krezel W, Chambon P, Haugen BR. Thyroid hormone resistance and increased metabolic rate in the RXR-gamma-deficient mouse. *J Clin Invest.* 2000;106:73–79.
34. Patsch JR, Prasad S, Gotto AM Jr, Patsch W. High density lipoprotein2. Relationship of the plasma levels of this lipoprotein species to its composition, to the magnitude of postprandial lipemia, and to the activities of lipoprotein lipase and hepatic lipase. *J Clin Invest.* 1987;80:341–347.
35. Blades B, Vega GL, Grundy SM. Activities of lipoprotein lipase and hepatic triglyceride lipase in postheparin plasma of patients with low concentrations of HDL cholesterol. *Arterioscler Thromb.* 1993;13: 1227–1235.
36. Rip J, Nierman MC, Wareham NJ, Luben R, Bingham SA, Day NE, van Miert JN, Hutten BA, Kastelein JJ, Kuivenhoven JA, Khaw KT, Boekholdt SM. Serum lipoprotein lipase concentration and risk for future coronary artery disease: the EPIC-Norfolk prospective population study. *Arterioscler Thromb Vasc Biol.* 2006;26:637–642.
37. Dowhan DH, Muscat GE. Characterization of the AB (AF-1) region in the muscle-specific retinoid X receptor-gamma: evidence that the AF-1 region functions in a cell-specific manner. *Nucleic Acids Res.* 1996;24:264–271.
38. Coon H, Myers RH, Borecki IB, Arnett DK, Hunt SC, Province MA, Djousse L, Leppert MF. Replication of linkage of familial combined hyperlipidemia to chromosome 1q with additional heterogeneous effect of apolipoprotein A-I/C-III/A-IV locus. The NHLBI Family Heart Study. *Arterioscler Thromb Vasc Biol.* 2000;20:2275–2280.
39. Elbein SC, Hoffman MD, Teng K, Leppert MF, Hasstedt SJ. A genome-wide search for type 2 diabetes susceptibility genes in Utah Caucasians. *Diabetes.* 1999;48:1175–1182.
40. van der Vleuten GM, Hijmans A, Kluijtmans LA, Blom HJ, Stalenhoef AF, de Graaf J. Thioredoxin interacting protein in Dutch families with familial combined hyperlipidemia. *Am J Med Genet A.* 2004;130:73–75.
41. Bodnar JS, Chatterjee A, Castellani LW, Ross DA, Ohmen J, Cavalcoli J, Wu C, Dains KM, Catanese J, Chu M, Sheth SS, Charugundla K, Demant P, West DB, de Jong P, Lusis AJ. Positional cloning of the combined hyperlipidemia gene Hyplip1. *Nat Genet.* 2002;30:110–116.
42. Pajukanta P, Lilja HE, Sinsheimer JS, Cantor RM, Lusis AJ, Gentile M, Duan XJ, Soro-Paavonen A, Naukkarinen J, Saarela J, Laakso M, Ehnholm C, Taskinen MR, Peltonen L. Familial combined hyperlipidemia is associated with upstream transcription factor 1 (USF1). *Nat Genet.* 2004;36:371–376.
43. Coon H, Xin Y, Hopkins PN, Cawthon RM, Hasstedt SJ, Hunt SC. Upstream stimulatory factor 1 associated with familial combined hyperlipidemia, LDL cholesterol, and triglycerides. *Hum Genet.* 2005;117: 444–451.
44. Huertas-Vazquez A, Aguilar-Salinas C, Lusis AJ, Cantor RM, Canizales-Quinteros S, Lee JC, Mariana-Nunez L, Riba-Ramirez RM, Jokiaho A, Tusie-Luna T, Pajukanta P. Familial combined hyperlipidemia in Mexicans: association with upstream transcription factor 1 and linkage on chromosome 16q24.1. *Arterioscler Thromb Vasc Biol.* 2005;25: 1985–1991.
45. Putt W, Palmen J, Nicaud V, Tregouet DA, Tahri-Daizadeh N, Flavell DM, Humphries SE, Talmud PJ. Variation in USF1 shows haplotype effects, gene : gene and gene : environment associations with glucose and lipid parameters in the European Atherosclerosis Research Study II. *Hum Mol Genet.* 2004;13:1587–1597.
46. Ng MC, Miyake K, So WY, Poon EW, Lam VK, Li JK, Cox NJ, Bell GI, Chan JC. The linkage and association of the gene encoding upstream stimulatory factor 1 with type 2 diabetes and metabolic syndrome in the Chinese population. *Diabetologia.* 2005;48:2018–2024.
47. Gibson F, Hercberg S, Froguel P. Common polymorphisms in the USF1 gene are not associated with type 2 diabetes in French Caucasians. *Diabetes.* 2005;54:3040–3042.
48. Zeggini E, Damcott CM, Hanson RL, Karim MA, Rayner NW, Groves CJ, Baier LJ, Hale TC, Hattersley AT, Hitman GA, Hunt SE, Knowler WC, Mitchell BD, Ng MC, O'Connell JR, Pollin TI, Vaxillaire M, Walker M, Wang X, Whittaker P, Xiang K, Jia W, Chan JC, Froguel P, Deloukas P, Shuldiner AR, Elbein SC, McCarthy MI. Variation within the gene encoding the upstream stimulatory factor 1 does not influence susceptibility to type 2 diabetes in samples from populations with replicated evidence of linkage to chromosome 1q. *Diabetes.* 2006;55:2541–2548.

CETP (cholesteryl ester transfer protein) promoter −1337 C > T polymorphism protects against coronary atherosclerosis in Japanese patients with heterozygous familial hypercholesterolaemia

Mutsuko TAKATA*, Akihiro INAZU†, Shoji KATSUDA*, Kenji MIWA*, Masa-aki KAWASHIRI*, Atsushi NOHARA‡, Toshinori HIGASHIKATA*, Junji KOBAYASHI§, Hiroshi MABUCHI‡ and Masakazu YAMAGISHI*

*Molecular Genetics of Cardiovascular Disorders, Graduate School of Medical Science, Kanazawa University, Takara-machi 13-1, Kanazawa 920-8641, Japan, †Department of Laboratory Science, Division of Health Sciences, Graduate School of Medical Science, Kanazawa University, Takara-machi 13-1, Kanazawa 920-8641, Japan, ‡Department of Lipidology, Kanazawa University, Takara-machi 13-1, Kanazawa 920-8641, Japan, and §Department for Lifestyle-related Diseases, Graduate School of Medical Science, Kanazawa University, Takara-machi 13-1, Kanazawa 920-8641, Japan

ABSTRACT

CETP (cholesteryl ester transfer protein) and HL (hepatic lipase) play a role in the metabolism of plasma lipoproteins, but the effects of *CETP* and *LIPC* (gene encoding HL) genotypes on coronary atherosclerosis may be dependent on LDL (low-density lipoprotein)-receptor activity. Recently, the −1337 C > T polymorphism in the *CETP* gene has been reported in REGRESS (Regression Growth Evaluation Statin Study) to be a major determinant of promoter activity and plasma CETP concentration. In the present study, we have investigated the effects of the *CETP* promoter −1337 C > T and *LIPC* promoter −514 C > T polymorphisms on serum lipid profiles and risk of coronary atherosclerosis in 206 patients (154 males) with heterozygous FH (familial hypercholesterolaemia). To evaluate coronary atherosclerosis, we used CSI (coronary stenosis index) calculated from coronary angiograms. The *CETP* −1337 T allele was less frequent in subjects with a CSI ⩾ 14 (mean value) in the group with coronary artery disease ($P = 0.04$, as determined by χ^2 test). ANOVA revealed that HDL-C (high-density lipoprotein-cholesterol) and triacylglycerol (triglyceride) levels were not significantly higher in the presence of the *CETP* promoter −1337 T allele. Combined with *LIPC* promoter polymorphisms, HDL-C levels were highest and CSI were lowest with *CETP* −1337 CT + TT and *LIPC* −514 CC genotypes, but a significant interaction was not shown. A multiple logistic regression analysis revealed that, in patients with coronary atherosclerosis, the *CETP* −1337 CC genotype was a significant genetic risk factor in FH (odds ratio = 2.022; $P = 0.0256$). These results indicate that the *CETP* promoter −1337C > T polymorphism is associated with the progression of coronary atherosclerosis in Japanese patients with FH, independent of HDL-C and triacylglycerol levels.

Key words: cholesteryl ester transfer protein (CETP), coronary artery disease, familial hypercholesterolaemia, hepatic lipase, single nucleotide polymorphism.

Abbreviations: AP, angina pectoris; Apo, apolipoprotein; BMI, body mass index; CAD, coronary artery disease; CETP, cholesteryl ester transfer protein; CSI, coronary stenosis index; FH, familial hypercholesterolaemia; HDL, high-density lipoprotein; HDL-C, HDL-cholesterol; HL, hepatic lipase; IDL, intermediate-density lipoprotein; LDL, low-density lipoprotein; LDL-C, LDL-cholesterol; MI, myocardial infarction; NCBI, National Center for Biotechnology Information; REGRESS, Regression Growth Evaluation Statin Study.

Correspondence: Dr Mutsuko Takata (email mutsuko9447@yahoo.co.jp).